# Exact Quickest Spectrum Sensing Algorithms for Eigenvalue-Based Change Detection

Martijn Arts, Andreas Bollig and Rudolf Mathar
Institute for Theoretical Information Technology
RWTH Aachen University
D-52074 Aachen, Germany
Email: {arts, bollig, mathar}@ti.rwth-aachen.de

***Abstract*—We study a collaborative quickest detection scheme that uses a function of the eigenvalues of the sample covariance matrix for a spectrum sensing system with a fusion center. A simple model consisting of one potentially present primary user (PU), which utilizes phase shift keying (PSK), and the standard additive white Gaussian noise (AWGN) assumption is considered. Here, for both detection hypothesis, the sample covariance matrix follows a Wishart distribution. For $K = 2$ collaborating secondary users (SUs), the probability distribution function (PDF) of the maximum-minimum eigenvalue (MME) test statistic can be derived analytically under both hypotheses, allowing us to develop exact quickest detection algorithms for known and unknown SNR. We analyze the two types of change detection problems in spectrum sensing, i.e., the channel becoming free when it was occupied before and vice versa. Performance evaluation is done by evaluating bounds and by comparing the presented quickest detection algorithms with the traditional block detection scheme.**

***Index Terms*—eigenvalue-based spectrum sensing, quickest detection, random matrix theory**

## I. Introduction

Opportunistic spectrum access has been proposed as a possible way to overcome the spectral scarcity problem by allowing unlicensed secondary users (SUs) to access unoccupied frequency bands. More precisely, the SUs decide autonomously whether to use a frequency band when its licensee, the so called primary users (PU), is not using [2]. The detection of such transmission opportunities is referred to as *spectrum sensing* and is a key requirement in order to minimize interference for the communication of the PUs. A variety of spectrum sensing algorithms have been reported in the literature and they can be differentiated by the signal features they exploit to perform the detection; see [3] for a review. Among these are detectors that are based on the sample covariance matrix and its eigenvalues, see, e.g., [3] for an overview. An advantage is that many of them do not require precise knowledge of the noise power, in contrast to the energy detector [4]. A well studied detector is the ratio of the maximum-to-minimum eigenvalue (MME) of the sample covariance matrix [5], which will be utilized in this work.

This work was partly supported by the Deutsche Forschungsgemeinschaft (DFG) project CoCoSa (grant MA 1184/26-1).

Parts of the results have been published in more detail as a pre-print in [1]. This is a revised version of the paper, which corrects some typographic errors. The original uncorrected version can be found in the conference proceedings.

Receiver noise is typically modeled as additive white Gaussian noise (AWGN) for theoretical analysis of the detectors. Under the AWGN assumption, when no PU is present, the sample covariance matrix is a so called Wishart matrix. *Random Matrix Theory* (RMT) studies the properties of random matrices and in the recent years significant progress on the exact eigenvalue distributions of Wishart matrices have been made, see for example [6] for a summary. Based on the joint ordered eigenvalue distribution, the distribution of the standard condition number (SCN) which is the test statistic of the MME detector, can be found [7], [8]. Consequently, this and other results from RMT have been applied to spectrum sensing [9].

Typically, *block detection* is applied in spectrum sensing scenarios. A block of consecutive samples is taken, the test statistic is computed and compared to a predefined threshold to form a decision about the occupancy status of a frequency band. However, the detection difficulty at hand does not influence the number of samples used for detection, since in block detection this number has to be predetermined and reflects a worst case point of view. Thus, even in the presence of a very strong PU signal, the decision can only be made after the necessary number of samples has been recorded. As we will discuss in more detail in Section IV, this may introduce significant delays that either result in interference for the PUs or reduce the potential transmittable amount of data of the SUs by shortening the transmission window.

Instead of applying block detection, the hypothesis test of identifying the channel occupancy can also be viewed as a *change* detection problem, c.f. Section IV. To minimize the mean detection delay of a hypothesis change while having a mean time to false alarm greater than a predefined constant is the goal of *quickest detection* [10], [11]. Quickest detection approaches have been investigated for spectrum sensing scenarios based on energy detection [12]–[14], using a sinusoidal PU signal [15] and exploiting cyclostationarity [16].

The remainder of the paper is organized as follows. In Section II we introduce the system model and notations. Probability density functions (PDFs) of the test statistic under both hypotheses are given in Section III by summarizing and extending results from literature. We discuss the two possible types of change detection problems in spectrum sensing in Section IV. Quickest eigenvalue-based spectrum sensing is introduced in Section V and algorithms for both types of

hypothesis changes in case of known and unknown SNR are derived and evaluated in Sections VI and VII, respectively.

## II. System Model

We consider the case of $K$ cooperating SUs, which share their collected samples with a fusion center that is responsible for the decision. The basic hypothesis testing problem of detecting the presence of a PU can be stated as follows:

$$\begin{aligned} \mathcal{H}_0 &: \mathbf{y}(t) = \mathbf{w}(t) \\ \mathcal{H}_1 &: \mathbf{y}(t) = \mathbf{x}(t) + \mathbf{w}(t)\,. \end{aligned} \tag{1}$$

Here, $\mathbf{y}(t)$ is a $K \times 1$ vector of complex baseband samples collected by the SUs at time index $t \in \mathbb{N} = \{1, 2, 3, \dots\}$. The vectors $\mathbf{w}(t)$ and $\mathbf{x}(t)$ stand for additive noise and the PU signal, respectively. The noise vector is assumed to be i.i.d. jointly complex circularly symmetric Gaussian distributed for each time index $t$ with no temporal correlation. More precisely, for each entry of the noise vector $\mathbf{w}$ the real- and imaginary part is independently Gaussian $\mathcal{N}(0, 1/2)$ distributed. For simplicity, we assume one PU is potentially present that is transmitting a deterministic phase shift keying (PSK) modulated signal, which is unknown to the SUs. It can be described as $\mathbf{x}(t) = \sqrt{\alpha}\, s(t)\, \mathbf{1}_K$, where $\alpha$ is the signal-to-noise ratio (SNR) of the receivers. The symbol $s(t) \in \mathbb{C}$ is a complex PSK symbol on the unit circle (i.e., $|s(t)| = 1$) and $\mathbf{1}_K$ is a column vector of dimension $K$ containing only ones. This is a very simple model of the $\mathcal{H}_1$ situation in which all SUs experience the same SNR. Nevertheless, it will allow us to give the exact detector PDF under $\mathcal{H}_1$, which will allow a fair comparison of block detection and quickest detection using the MME detector.

In order to estimate the covariance matrix, a block of $N$ time instances is considered. The block of samples can be written as a $K \times N$ matrix: $\mathbf{Y} = [\mathbf{y}(1), \mathbf{y}(2), \dots, \mathbf{y}(N)]$. Analogously, a signal matrix $\mathbf{X}$ and a noise matrix $\mathbf{W}$ can be constructed. Hence, it follows $\mathbf{Y} = \mathbf{W}$ under $\mathcal{H}_0$ and $\mathbf{Y} = \mathbf{X} + \mathbf{W}$ under $\mathcal{H}_1$. Using this notation, we can calculate the sample covariance matrix as $\mathbf{R}_y = \frac{1}{N}\mathbf{Y}\mathbf{Y}^{\mathbf{H}}$. It converges to the statistical covariance matrix for $N \to \infty$. The test statistic of the well known MME detector is:

$$T = \frac{\lambda_1}{\lambda_K}, \tag{2}$$

where $\lambda_1 \geq \cdots \geq \lambda_K$ are the ordered eigenvalues of the sample covariance matrix $\mathbf{R}_y$ [5]. Since scaling of the sample covariance matrix results in the same scaling of its eigenvalues, the ratio is not affected by it. Thus, we will omit the normalization factor and use the scaled sample covariance matrix $\mathbf{R} = \mathbf{Y}\mathbf{Y}^{\mathbf{H}}$ in the following. This holds analogously for the noise power, which is why the system model depends on the SNR directly.

We assume the SUs are *dual radio* transceivers (see [2]), meaning that they can simultaneously transceive on one band and receive samples on another. Assuming the PU uses his whole frequency band when he is present, the SU may only use a part of this frequency band for spectrum sensing. In doing so, the SUs may transmit on the remaining part of the band when it is free, while monitoring the other part for a change $\mathcal{H}_0$ to $\mathcal{H}_1$. Section IV discusses the importance of this hypothesis change for spectrum sensing.

## III. Exact MME Detector PDFs

In this section, the distribution of the sample covariance matrix is specified under both hypotheses. For the case of $K = 2$ SUs the PDFs of the test statistic can be found exactly. Hence, the remainder of the paper will assume that $K = 2$. Numerically evaluating the PDFs for $K \geq 2$ may be possible by utilizing results from [8] but this is out of the scope of this paper.

### A. PDF under $\mathcal{H}_0$

Under hypothesis $\mathcal{H}_0$, the sample covariance matrix can be written as $\mathbf{R}_0 = \mathbf{W}\mathbf{W}^{\mathbf{H}}$, which is a complex uncorrelated central Wishart matrix of dimension $K$ with $N$ degrees of freedom [17]. We denote this as $\mathbf{R}_0 \sim \mathcal{CW}_K(N, \mathbf{I}_K)$. For $K = 2$ the PDF of the MME detector from (2) can be given exactly for $T \geq 1$ as [7]

$$f_0(T) = \frac{(N-1)\Gamma(2N)}{[\Gamma(N)]^2} \frac{(T-1)^2\, T^{(N-2)}}{(T+1)^{2N}}. \tag{3}$$

### B. PDF under $\mathcal{H}_1$

Under hypothesis $\mathcal{H}_1$, the sample covariance matrix is given by

$$\mathbf{R}_1 = (\mathbf{X} + \mathbf{W})(\mathbf{X} + \mathbf{W})^{\mathbf{H}} \tag{4}$$

$$= \sum_{j=1}^{N} (\mathbf{x}_j + \mathbf{w}_j)(\mathbf{x}_j + \mathbf{w}_j)^{\mathbf{H}} = \sum_{j=1}^{N} \mathbf{y}_j (\mathbf{y}_j)^{\mathbf{H}}\,, \tag{5}$$

where the $j$-th column of the sample matrix $\mathbf{y}_j$ follows a complex circularly symmetric Gaussian distribution with mean $\mathbf{x}_j$, i.e., $\mathbf{y}_j \sim \mathcal{CN}(\mathbf{x}_j, \mathbf{I}_K)$ for all $j = 1, \dots, N$. Hence, it is a complex uncorrelated non-central Wishart distribution with dimension $K$, having $N$ degrees of freedom with non-centrality matrix $\mathbf{\Omega} = \mathrm{E}[\mathbf{Y}]\mathrm{E}[\mathbf{Y}]^{\mathbf{H}} = \alpha N\, \mathbf{1}_K \mathbf{1}_K^{\mathbf{T}}$ (c.f. [17]). In short notation we write $\mathbf{R}_1 \sim \mathcal{CW}_K(N, \mathbf{I}_K, \mathbf{\Omega})$.

In [8] the MME detector PDF was reported in a MIMO beamforming context for the case that $K = N = 2$. Following the same way as reported there and using straightforward tedious algebra, we can generalize the result to arbitrary $N$. For this, we collect the ordered eigenvalues of $\mathbf{R}_1$ and $\mathbf{\Omega}$ in the vectors $\boldsymbol{\lambda} = (\lambda_1, \lambda_2)^{\mathbf{T}}$ and $\boldsymbol{\omega} = (\omega_1, \omega_2)^{\mathbf{T}}$, respectively. For $K = 2$, $T \geq 1$ and $\omega_1 \neq \omega_2$ we arrive at (6). Noticing that $\mathbf{\Omega}$ is a rank one matrix, we can find its eigenvalues directly as $\omega_1 = 2\alpha N$ and $\omega_2 = 0$. Inserting the values for $\omega_1$ and $\omega_2$ into (6), we gain a simplified version of the PDF in (7). Although (7) contains an infinite sum it can be evaluated precisely by noting that for high $j$ the contribution of the summands becomes negligible. An example plot of both $f_0$ and $f_1$ is shown in Figure 1.

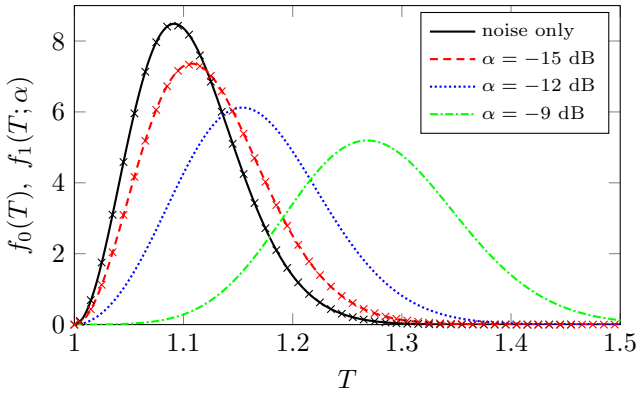


Fig. 1. Plot of $f_0(T)$ (noise only) in black and $f_1(T;\alpha)$ for different values of the SNR $\alpha$ indicated by different colors. The number of samples is $N = 500$. Crosses indicate values taken from an empirical PDF obtained by simulation.

## IV. Change Detection in Spectrum Sensing

In spectrum sensing, two types of hypothesis change can be distinguished. Firstly, a change from $\mathcal{H}_0$ to $\mathcal{H}_1$ and secondly a change from $\mathcal{H}_1$ to $\mathcal{H}_0$. Both situations are depicted in Figure 2 and relevant time points with associated delays are described.

The delay introduced by the detection algorithm has different practical implications depending on the type of hypothesis change considered. In the case that a previously occupied frequency band becomes free again ($\mathcal{H}_1$ to $\mathcal{H}_0$), the detection delay shortens the transmission window for the SUs. This represents an inefficiency of the secondary system, but has no direct negative effect on the primary system. However, if the channel is falsely declared to be free and the secondary system accesses it, interference for the primary system is inevitable. Thus, this change is critical with respect to detection accuracy. If we consider the change from $\mathcal{H}_0$ to $\mathcal{H}_1$, a PU appears that intends to start a transmission. Here, the detection delay translates to increased interference for the primary system, since the secondary system does not immediately terminate its communication on this band. Thus, it is the more critical case as far as the detection delay is concerned, since it has a direct negative effect on the (licensed) primary system.

## V. Quickest Eigenvalue-Based Spectrum Sensing

In contrast to block detection, where the goal is to decide which hypothesis is true in a block of samples, quickest detection (QD) has the objective to minimize the detection delay of a change between two hypotheses. Let us assume (without loss of generality) that before the unknown change time $t_\mathrm{c}$ hypothesis $\mathcal{H}_0$ is true and that it changes to $\mathcal{H}_1$ at $t_\mathrm{c}$ (c.f. Figure 2). In QD it is usually presumed that the samples taken by the detection algorithm are i.i.d. random variables, where at $t_\mathrm{c}$ the underlying distribution changes. For each sample the detection algorithm updates its output value and compares it to a predefined threshold $h_G$. An alarm is raised if the threshold $h_G$ is exceeded. If the threshold was not surpassed after a predetermined maximum run-time, the algorithm is aborted and restarted in order to avoid generating false alarms.

The estimation of the covariance matrix requires taking a block of samples. To use a function of the eigenvalues of the sample covariance matrix as an input to a QD algorithm, we must introduce a time-dependent version of the test statistic $T$, i.e., $T(k) = \frac{\lambda_1(k)}{\lambda_K(k)}$, where in our case $K = 2$. Blocks of $N$ non-overlapping consecutive samples are taken to calculate the $k$-th sample covariance matrix $\mathbf{R}(k) = \mathbf{Y}(k)(\mathbf{Y}(k))^\mathbf{H}$, where $\mathbf{Y}(k) = [\mathbf{y}((k-1)N+1),\ \cdots, \mathbf{y}(kN)]$.

For the theoretical treatment we make an additional assumption that no hypothesis change may happen within a block, that is $t_\mathrm{c} \in \{(k-1)N+1 \mid k \in \mathbb{N}\}$. Note, that this assumption is a standard one for the analysis of block detection algorithms. Then, depending on whether $T(k)$ was observed before or after $t_\mathrm{c}$ it is distributed according to $f_0(T)$ or $f_1(T;\alpha)$, respectively.

The most widely known QD algorithm is called the cumulative sum (CUSUM) algorithm. It exploits that the log-likelihood ratio (LLR), defined as $l(k) = \log\left(\frac{f_1(T(k))}{f_0(T(k))}\right)$, is positive on average when $\mathcal{H}_1$ is true and negative on average when $\mathcal{H}_0$ is true. The idea behind the CUSUM is that a cumulative sum of the LLR will show a positive drift under $\mathcal{H}_1$. However, accumulating a negative drift will increase the detection delay. Given the definitions from above, the CUSUM can be (recursively) formulated as follows [10], [18]:

$$g(k) = \max_{0\le m\le k} \sum_{j=m+1}^{k} \log\left(\frac{f_1(T(j);\alpha)}{f_0(T(j))}\right) \tag{8}$$

$$= [g(k-1) + l(k)]^+ , \tag{9}$$

with $g(0) = 0$ and $[\cdot]^+ = \max(\cdot, 0)$. Note, that both PDFs $f_0(T)$ and $f_1(T;\alpha)$ must be known.

The relevant performance measures for QD are the mean time to false alarm $\bar{\tau}_\mathrm{fa} = \mathrm{E}_{f_0}[t_\mathrm{a}]$ and the mean detection delay $\bar{\tau}_\mathrm{d} = \mathrm{E}_{f_1}\left[t_\mathrm{a} - t_\mathrm{c} + 1 \,|\, t_\mathrm{a} \ge t_\mathrm{c}, \mathcal{T}_1^{(t_\mathrm{c}-1)}\right]$, where the trajectory of the observations before $t_\mathrm{c}$ is denoted as $\mathcal{T}_1^{(t_\mathrm{c}-1)} = [T(1), \ldots, T(t_\mathrm{c}-1)]$ [10]. The notation $\mathrm{E}_f[\cdot]$ stands for the expectation over the PDF $f$.

## VI. Exact Eigenvalue-Based Quickest Detection Algorithms for $\mathcal{H}_0$ to $\mathcal{H}_1$

For this section, we use the results from Section III and the detection scheme from Section V to give an exact eigenvalue-based QD algorithm tailored to detect the change $\mathcal{H}_0$ to $\mathcal{H}_1$ for the model from Section II. As argued in Section IV, this is the more critical of the two possible types of changes, since the delay directly influences interference for the primary system. Both the case of known and unknown SNR $\alpha$ are investigated and the performance is evaluated with respect to the MME block detector operating on the same model.

### A. Known SNR

Under the model from Section II both PDFs of the MME test statistic from (2) were given in Section III. So when the SNR $\alpha$ is known, the CUSUM algorithm from (9) can directly be applied. Explicitly inserting both (3) and (7) into the LLR $l(k)$ and simplifying yields (10). There, we made use of the

$$f_1(T;\boldsymbol{\omega}) = \frac{e^{-(\omega_1+\omega_2)}\,(T-1)T^{(N-2)}}{(\omega_1-\omega_2)} \sum_{j=0}^{\infty}\sum_{l=0}^{\infty} \frac{\Gamma(j+l+2N-1)\,T^j\left(\omega_1^j\omega_2^l-\omega_2^j\omega_1^l\right)}{j!\,l!\,\Gamma(j+N-1)\,\Gamma(l+N-1)(T+1)^{(j+l+2N-1)}} \tag{6}$$

$$f_1(T;\alpha) = e^{-(2\alpha N)}\,(T-1)T^{(N-2)} \sum_{j=0}^{\infty} \frac{(T^j-1)\,\Gamma(j+2N-1)\,(2\alpha N)^{(j-1)}}{j!\,\Gamma(j+N-1)\,\Gamma(N-1)\,(T+1)^{(j+2N-1)}} \tag{7}$$

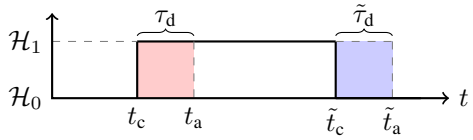


Fig. 2. Change detection problems in spectrum sensing. At $t_\mathrm{c}$ a change from Hypothesis $\mathcal{H}_0$ (unoccupied channel) to Hypothesis $\mathcal{H}_1$ (occupied channel) occurs. The detection algorithm raises an alarm at $t_\mathrm{a}$, so the detection delay is $\tau_\mathrm{d} = t_\mathrm{a} - t_\mathrm{c}$. The reverse situation that an occupied channel becomes free happens at $\tilde{t}_\mathrm{c}$ with analogously defined alarm time $\tilde{t}_\mathrm{a}$ and detection delay $\tilde{\tau}_\mathrm{d}$. The duration shaded in red indicates interference for the primary system, while the duration in blue symbolizes wasted transmission opportunities for the secondary system.

Pochhammer symbol $(a)_b = (a+b-1)!/(a-1)!$.

To assess the detection performance beforehand and to ease determination of a proper threshold $h_G$, bounds on $\bar{\tau}_\mathrm{d}$ and $\bar{\tau}_\mathrm{fa}$ are helpful.

An upper bound on $\bar{\tau}_\mathrm{d}$ can be found in [10]:

$$\bar{\tau}_\mathrm{d} \leq \bar{\tau}_\mathrm{d}^\star \leq \frac{(h+\gamma_{f_1})}{\mathrm{E}_{f_1}\left[l(k)\right]}\,, \tag{11}$$

where

$$\gamma_f = \sup_{\delta>0}\,\mathrm{E}_f\left[l(k)-\delta \mid l(k)\geq\delta>0\right] \tag{12}$$

and

$$\bar{\tau}_\mathrm{d}^\star = \sup_{t_\mathrm{c}\geq 1}\operatorname{ess\,sup}\mathrm{E}_{f_1}\left[t_\mathrm{a}-t_\mathrm{c}+1\,|\,t_\mathrm{a}\geq t_\mathrm{c}, \mathcal{T}_1^{(t_\mathrm{c}-1)}\right] \tag{13}$$

is the worst mean delay [19].

Likewise, a lower bound on $\bar{\tau}_\mathrm{fa}$ can be found in [10]:

$$\bar{\tau}_\mathrm{fa} \geq \frac{1}{\mathrm{E}_{f_0}\left[l(k)\right]}\left(\frac{e^{-\varphi_{f_0}h}-1}{\varphi_{f_0}}+h+\gamma_{f_0}\right)\,, \tag{14}$$

where $\varphi_f$ is the single non-zero root of $\mathrm{E}_f[e^{-\varphi_f\,l(k)}]=1$. For $\varphi_{f_0}$, the following equation must be solved:

$$\mathrm{E}_{f_0}[e^{-\varphi_{f_0}\,l(k)}] = \int_1^\infty \left(\frac{f_1(T;\alpha)}{f_0(T)}\right)^{-\varphi_{f_0}} f_0(T)\,\mathrm{d}T \stackrel{!}{=} 1\,. \tag{15}$$

Obviously, $\varphi_{f_0}=-1$ solves (15), since only the integral over $f_1(T;\alpha)$ remains. Thus, (14) can easily be simplified to:

$$\bar{\tau}_\mathrm{fa} \geq \frac{1}{\mathrm{E}_{f_0}\left[l(k)\right]}\left(1-e^h+h+\gamma_{f_0}\right)\,. \tag{16}$$

A second, much simpler bound is [10]:

$$\bar{\tau}_\mathrm{fa} \geq e^h\,. \tag{17}$$

Unfortunately, neither $\mathrm{E}_{f_0}\left[l(k)\right]$ nor $\mathrm{E}_{f_1}\left[l(k)\right]$, $\gamma_{f_0}$ or $\gamma_{f_1}$ can be handled analytically, but numerical evaluation is possible.

In Figures 3a and 3b results of a Monte-Carlo simulation of the CUSUM algorithm for $\bar{\tau}_\mathrm{fa}$ and $\bar{\tau}_\mathrm{d}$ are depicted together with the corresponding theoretical bounds from (11), (16) and (17) are depicted. While here, the bound from (17) is tighter than (16), we have observed the opposite situation when considering smaller numbers of samples $N$.

### *B. Unknown SNR*

Let us assume that the SNR $\alpha$ is unknown to the SUs, which is a more realistic scenario in spectrum sensing. Then, direct application of the CUSUM algorithm is not possible. Performing likelihood ratio tests when parameters are unknown can be done by utilizing a generalized likelihood ratio test (GLRT). There the unknown parameters are estimated beforehand by maximum likelihood estimation (MLE) [20]. Here, the only unknown parameter is $\alpha$ and we can use the GLRT to extend the CUSUM algorithm from (8). The resulting generalized likelihood ratio (GLR) algorithm can be given as [10]:

$$g_G(k) = \max_{0\leq m\leq k}\sup_{\hat{\alpha}}\sum_{j=m+1}^{k}\log\left(\frac{f_1(T(j);\hat{\alpha})}{f_0(T(j))}\right)\,. \tag{18}$$

The supremum present in (18) has to be evaluated numerically, since we are not aware of an analytical form for the MLE of $\alpha$ in $f_1$. Also the GLR has a higher complexity than the CUSUM, since it cannot be formulated recursively and demands storage of all previous samples.

Firstly, the mean time to false alarm $\bar{\tau}_\mathrm{fa}$ gained from a simulation for both the GLR and the CUSUM algorithm is shown in Figure 3a. Secondly, the mean time to detection $\bar{\tau}_\mathrm{d}$ obtained from a simulation for both algorithms is plotted in Figure 3b. Note also, that in both plots the corresponding bounds from (11), (16) and (17), which are only valid for the CUSUM, are depicted as well. Moreover, the thresholds which result in the same $\bar{\tau}_\mathrm{fa}$ for both algorithms are shown in both Figures 3a and 3b. This helps to visualize the increase in detection delay of the GLR with respect to the CUSUM, which is due to the fact that the GLR performs an estimation of the SNR.

Next, we compare the performance of the GLR algorithm to the performance of a MME block detector. For the latter, we can directly predict the probability of detection $P_\mathrm{d}(h) = 1-\int_1^h f_1(T;\alpha)\,\mathrm{d}T$ and the probability of false alarm $P_\mathrm{fa}(h) = 1-\int_1^h f_0(T)\,\mathrm{d}T$ for a given threshold with the help of (3) and (7). We designed the MME block detector with a block length of $10^5$ samples with $P_\mathrm{fa}=0.015$ resulting in the threshold $h=1.0146$, which exhibits $P_\mathrm{d}=0.928$ for an SNR $\alpha=-20$ dB. For the GLR, a Monte-Carlo simulation

$$l(k) = \log\left(\frac{f_1(T(k);\alpha)}{f_0(T(k))}\right) = \log\left(\frac{e^{-2\alpha N}}{(T(k)-1)}\sum_{j=0}^{\infty}\frac{(T(k)^j-1)\,(2\alpha N)^{(j-1)}\;(2N)_{(j-1)}}{j!\,(T(k)+1)^{(j-1)}\;(N)_{(j-1)}}\right) \tag{10}$$

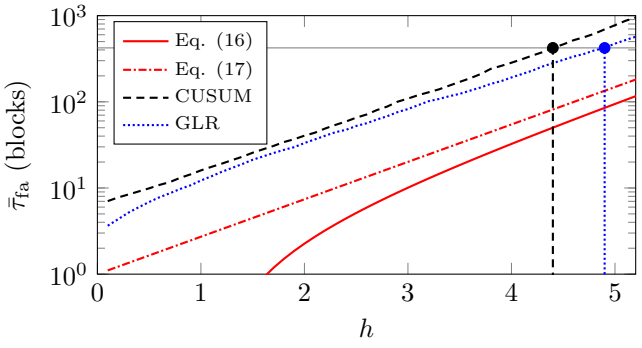


(a) Mean time to false alarm $\bar{\tau}_{\text{fa}}$.

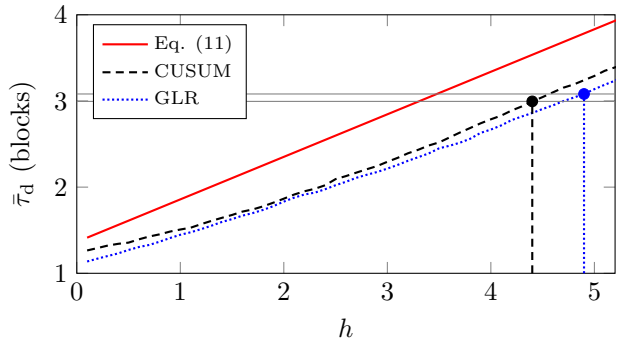


(b) Mean time to detection $\bar{\tau}_{\text{d}}$.

Fig. 3. Performance of the GLR (blue) and the CUSUM (black) including the theoretical bounds for the CUSUM from (11), (16) and (17) (red). The simulated performance of both the CUSUM and GLR algorithm is shown for $N = 10000$ and SNR $\alpha = -17$ dB, where the GLR numerically evaluates the supremum over $\hat{\alpha}$ within the interval $[-20.5, -5]$ dB in 0.1 dB steps. The gray vertical lines mark an exemplary choice of thresholds for which both algorithms exhibit the same $\bar{\tau}_{\text{fa}}$. This helps to visualize the performance loss of the GLR with respect to $\bar{\tau}_{\text{d}}$ in Figure 3b due to the SNR estimation.

with $N = 10000$ for 1000 random seeds was performed that includes a variety of thresholds and the supremum in (18) was numerically evaluated in the range $[-20.5, -5]$ dB in 0.1 dB steps. In Figure 4 the probability of false alarm $P_{\text{fa}}$ and the probability of detection $P_{\text{d}}$ over the run-time of the GLR is depicted for several SNRs. There, a threshold $h_G = 4.5$ was chosen, such that at a run-time of 10 blocks (which is equal to having $10^5$ samples processed) the $P_{\text{fa}}$ for the GLR is equal to the $P_{\text{fa}}$ for which the MME block detector was designed. For a wide range of SNRs the GLR quickest detection algorithm offers faster detection than the MME block detector at comparable or even lower false alarm rate. However, at very low SNRs the MME block detector offers a quicker and more reliable detection. This can be explained by the fact that the MME block detector processes the entirety of samples (in this case $10^5$ samples) to form a decision and was designed to perform well in the worst case. In contrast, the GLR subsequently processes blocks of $N = 10000$ samples to estimate the sample covariance matrix, thereby aiming at

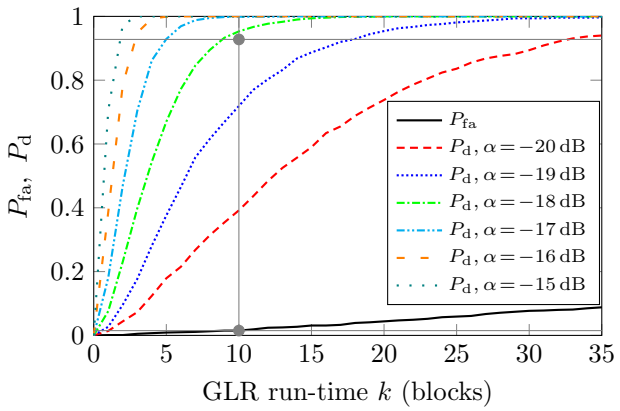


Fig. 4. Performance of the GLR algorithm, evaluated as $P_{\text{d}}$ and $P_{\text{fa}}$ over the algorithm run-time for the threshold $h = 4.5$. For $P_{\text{d}}$ different SNRs were considered as indicated by the different colors. The gray circular markers and the thin solid lines indicate the performance of the MME block detector designed for a block length of $10^5$ samples and $P_{\text{fa}} = 0.015$, which results in $P_{\text{d}} = 0.928$ at SNR $\alpha = -20$ dB.

reducing the detection delay. In practical scenarios, the SNR $\alpha$ after the hypothesis change can be considered to lie in a certain interval, say, e.g., $[-5, -20]$ dB. Then, the GLR algorithm will offer faster detection in the average case, while being slower in the worst case. Thus, when choosing $N$ for the GLR algorithm, one has to trade-off the average detection delay versus the worst case SNR performance gap compared to the block detection approach.

In summary, for a wide range of SNRs the presented GLR quickest detection algorithm offers faster detection of the appearance of a PU and consequently the possibility to free the channel earlier resulting in reduced interference for the primary system. However, the MME block detector is faster in detecting very weak PU signals close to the worst case SNR for which it was designed.

## VII. Exact Eigenvalue-Based Quickest Detection Algorithms for $\mathcal{H}_1$ to $\mathcal{H}_0$

This section studies the second kind of possible hypothesis change ($\mathcal{H}_1$ to $\mathcal{H}_0$), where the detection delay is associated with inefficiency in the secondary system and detection accuracy is critically linked to primary system interference as discussed in Section IV.

### A. Known SNR

To detect a change from $\mathcal{H}_1 \rightarrow \mathcal{H}_0$ the inverse situation of Section VII must be considered. Thus, the LLR in this case is $\tilde{l}(k) = \log\left(\frac{f_0(T(k))}{f_1(T(k);\alpha)}\right) = -l(k)$. Hence, the CUSUM algorithm for this case directly follows as $\tilde{g}(k) = [\tilde{g}(k-1) - l(k)]^+$. Similarly, the bounds presented in (11) and (16) can be adapted straightforwardly by inserting $\tilde{l}(k)$ for $l(k)$ and by exchanging $f_0$ with $f_1$ and vice versa.

### B. Unknown SNR

Since numerator and denominator are swapped in the LLR $\tilde{l}(k)$ also the GLR has to be adapted. Now, the MLE for the unknown SNR concerns the denominator. Hence, the supremum in (18) must be exchanged with an infimum and a negative sign can be factored out of the sum such that the LLR from (10) can be utilized directly. The GLR for the $\mathcal{H}_1$ to $\mathcal{H}_0$ case then yields:

$$\tilde{g}_G(k) = \max_{0\leq m\leq k} \inf_{\hat{\alpha}} -\sum_{j=m+1}^{k} \log\left(\frac{f_1(T(j);\hat{\alpha})}{f_0(T(j))}\right) . \qquad (19)$$

In Figure 5 we perform the analogous comparison to Figure 4 for the $\mathcal{H}_1$ to $\mathcal{H}_0$ change. Due to the inverted situation the false alarm performance is now dependent on the SNR and the detection performance is constant, contrary to the $\mathcal{H}_0$ to $\mathcal{H}_1$ case. Because of that, the advantage of the quickest detection approach that was observed in Section VI is not present here. We conclude, that for this type of hypothesis change the block detection approach is faster and more reliable in terms of detection accuracy.

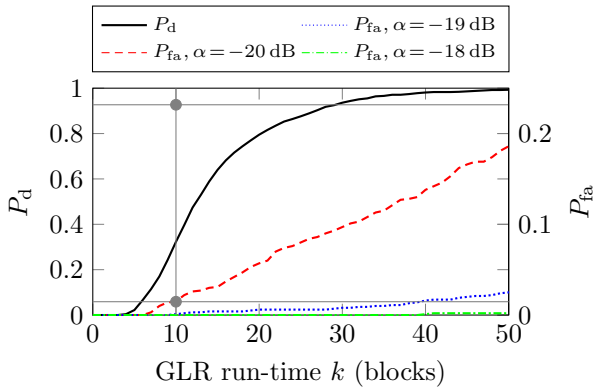


Fig. 5. Performance of the GLR algorithm from (19), evaluated as $P_\mathrm{d}$ and $P_\mathrm{fa}$ over the algorithm run-time for the threshold $h = 2.4$. Note, that $P_\mathrm{d}$ is plotted on the left ordinate and $P_\mathrm{fa}$ is plotted on the right ordinate for different SNRs. The gray circular markers and the thin solid lines indicate the performance of the MME block detector also designed to detect the change from $\mathcal{H}_1$ to $\mathcal{H}_0$ for a block length of $10^5$ samples and $P_\mathrm{fa} = 0.015$ at SNR $\alpha = -20$ dB, which results in $P_\mathrm{d} = 0.9117$.

## VIII. Conclusion

In this work, we have studied a collaborative quickest eigenvalue-based spectrum sensing system with a fusion center. We have introduced a basic AWGN system model with $K$ collaborating SUs and a single PU. The PU transmits PSK signals and the SUs have identical SNRs. Under this model, both the noise only ($\mathcal{H}_0$) hypothesis and the PU signal + noise ($\mathcal{H}_1$) hypothesis lead to Wishart sample covariance matrices. Thus, confining the number of SUs to $K = 2$ we can give the exact PDF of the maximum-minimum eigenvalue (MME) test statistic under both hypotheses. The two relevant change detection problems in spectrum sensing were separately investigated, i.e., $\mathcal{H}_0$ to $\mathcal{H}_1$ and $\mathcal{H}_1$ to $\mathcal{H}_0$. For both cases, exact quickest detection algorithms were given for known and unknown SNR. Performance evaluation was performed by comparing to the traditional block detection scheme. It was found, that for the $\mathcal{H}_0$ to $\mathcal{H}_1$ change, where detection delay is directly associated with primary system interference, the quickest detection approach is applicable. It offers reduced detection delay at similar or better false alarm performance for a wide range of SNRs. For the second type of change ($\mathcal{H}_1$ to $\mathcal{H}_0$) the traditional block detection algorithm was found to be the more sensible choice. Future work should aim at generalizing to more realistic models with channel fading and more secondary users.

## References


[1] M. Arts, A. Bollig, and R. Mathar, "Quickest Eigenvalue-Based Spectrum Sensing using Random Matrix Theory," *ArXiv e-prints arXiv:1504.01628 [cs.IT]*, Apr. 2015.

[2] Q. Zhao and B. M. Sadler, "A survey of dynamic spectrum access," *IEEE Signal Processing Magazine*, vol. 24, no. 3, pp. 79–89, 2007.

[3] E. Axell, G. Leus, E. G. Larsson, and H. V. Poor, "Spectrum sensing for cognitive radio: State-of-the-art and recent advances," *IEEE Signal Processing Magazine*, vol. 29, no. 3, pp. 101–116, 2012.

[4] A. Sonnenschein and P. Fishman, "Radiometric detection of spread-spectrum signals in noise of uncertain power," *IEEE Transactions on Aerospace and Electronic Systems*, vol. 28, pp. 654–660, July 1992.

[5] Y. Zeng and Y.-C. Liang, "Maximum-minimum eigenvalue detection for cognitive radio," in *IEEE 18th Annual International Symposium on Personal, Indoor and Mobile Radio Communication*, vol. 7, (Athens, Greece), pp. 1–5, 2007.

[6] A. Zanella, M. Chiani, and M. Z. Win, "On the marginal distribution of the eigenvalues of Wishart matrices," *IEEE Transactions on Communications*, vol. 57, no. 4, pp. 1050–1060, 2009.

[7] A. Kortun, T. Ratnarajah, M. Sellathurai, C. Zhong, and C. Papadias, "On the Performance of Eigenvalue-Based Cooperative Spectrum Sensing for Cognitive Radio," *IEEE Journal of Selected Topics in Signal Processing*, vol. 5, pp. 49–55, Feb. 2011.

[8] M. Matthaiou, M. McKay, P. Smith, and J. Nossek, "On the condition number distribution of complex wishart matrices," *IEEE Transactions on Communications*, vol. 58, pp. 1705–1717, June 2010.

[9] W. Zhang, G. Abreu, M. Inamori, and Y. Sanada, "Spectrum Sensing Algorithms via Finite Random Matrices," *IEEE Transactions on Communications*, vol. 60, pp. 164–175, Jan. 2012.

[10] M. Basseville and I. V. Nikiforov, *Detection of abrupt changes: theory and application*. Englewood Cliffs: Prentice Hall, 1993.

[11] H. V. Poor and O. Hadjiliadis, *Quickest detection*, vol. 40. Cambridge University Press Cambridge, 2009.

[12] L. Lai, Y. Fan, and H. V. Poor, "Quickest detection in cognitive radio: A sequential change detection framework," in *IEEE Global Telecommunications Conference (GLOBECOM)*, (New Orleans, USA), pp. 1–5, 2008.

[13] S. Zarrin and T. J. Lim, "Cooperative quickest spectrum sensing in cognitive radios with unknown parameters," in *IEEE Global Telecommunications Conference (GLOBECOM)*, (Honululu, Hawaii, USA), pp. 1–6, IEEE, 2009.

[14] E. Hanafi, P. A. Martin, P. J. Smith, and A. J. Coulson, "Extension of Quickest Spectrum Sensing to Multiple Antennas and Rayleigh Channels," *IEEE Communications Letters*, vol. 17, no. 4, pp. 625–628, 2013.

[15] H. Li, C. Li, and H. Dai, "Quickest spectrum sensing in cognitive radio," in *IEEE 42nd Annual Conference on Information Sciences and Systems (CISS)*, (Princeton, USA), pp. 203–208, 2008.

[16] H. Li, "Cyclostationary feature based quickest spectrum sensing in cognitive radio systems," in *IEEE 72nd Vehicular Technology Conference Fall (VTC 2010-Fall)*, (Ottawa, Canada), pp. 1–5, 2010.

[17] A. T. James, "Distributions of matrix variates and latent roots derived from normal samples," *The Annals of Mathematical Statistics*, vol. 35, no. 2, pp. 475–501, 1964.

[18] E. S. Page, "Continuous inspection schemes," *Biometrika*, vol. 41, no. 1/2, pp. 100–115, 1954.

[19] G. Lorden, "Procedures for reacting to a change in distribution," *The Annals of Mathematical Statistics*, vol. 42, no. 6, pp. 1897–1908, 1971.

[20] S. M. Kay, *Fundamentals of statistical signal processing: detection theory*, vol. II. Upper Saddle River: Prentice Hall, 1998.